

Supporting Information:

**Probing strongly exchange coupled magnetic behaviors in soft/hard Ni/CoFe₂O₄
core/shell nanoparticles**

J. K. Han¹, A.A. Baker¹, J.R.I. Lee¹, S.K. McCall¹

1. Critical Materials Institute, Lawrence Livermore National Laboratory,
Livermore, California 94550, U.S.A

Corresponding Author: Jinkyu Han (han10@llnl.gov)

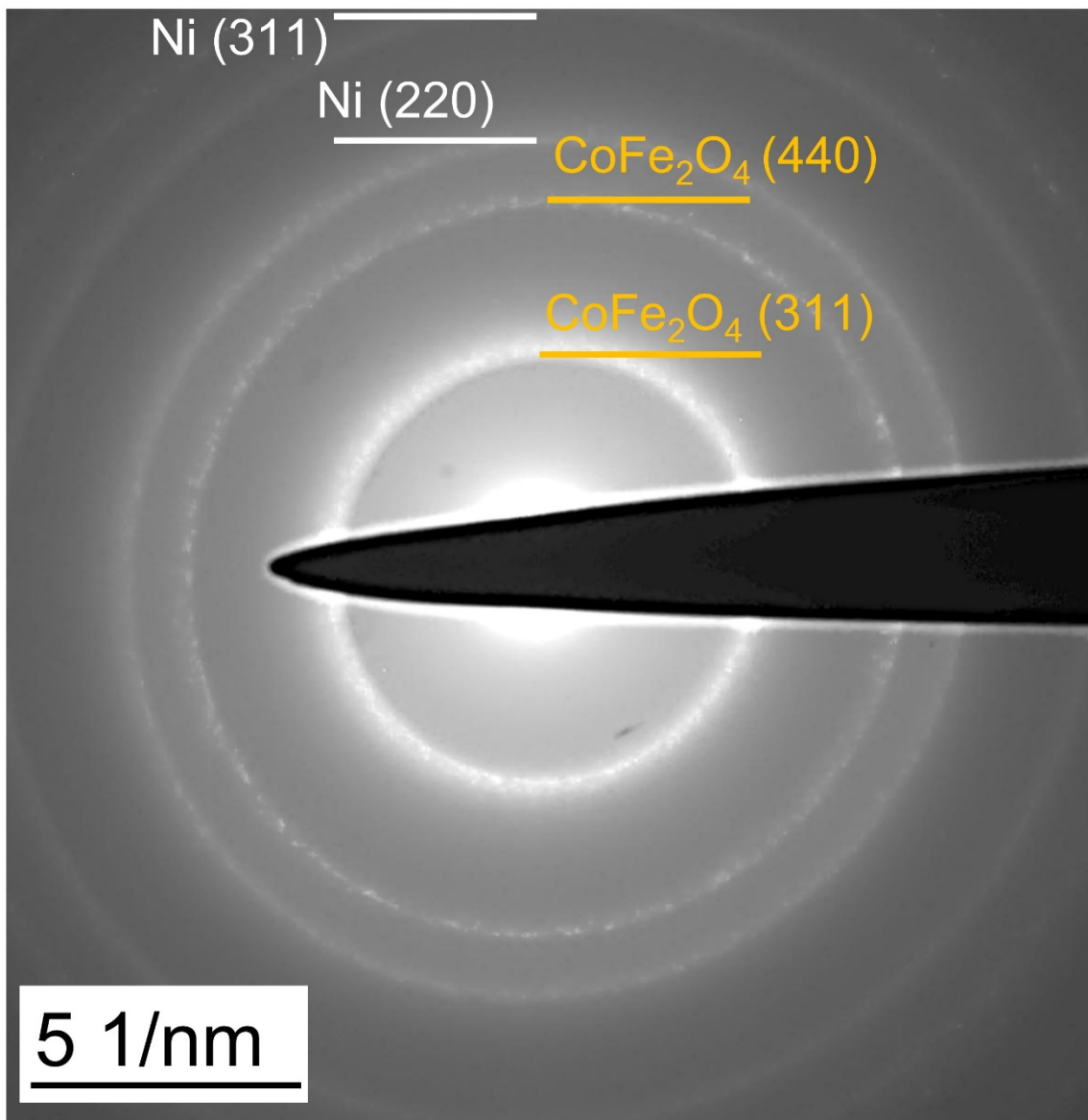


Figure S1. SAED patterns of resulting Ni/CoFe₂O₄ core/shell nanoparticles. The indices match well with observed and theoretical values [1,2].

Table S1. Interplanar distance comparison estimated from SAED pattern in Figure S1 and theoretical values from literatures.

	Estimated from SAED pattern	Theoretical values
$d_{\text{CoFe}_2\text{O}_4} (311)$	0.253 nm	0.253 nm [1]
$d_{\text{CoFe}_2\text{O}_4} (440)$	0.147 nm	0.148 nm [1]
$d_{\text{Ni}} (220)$	0.126 nm	0.125 nm [2]
$d_{\text{Ni}} (311)$	0.103 nm	0.106 nm [2]

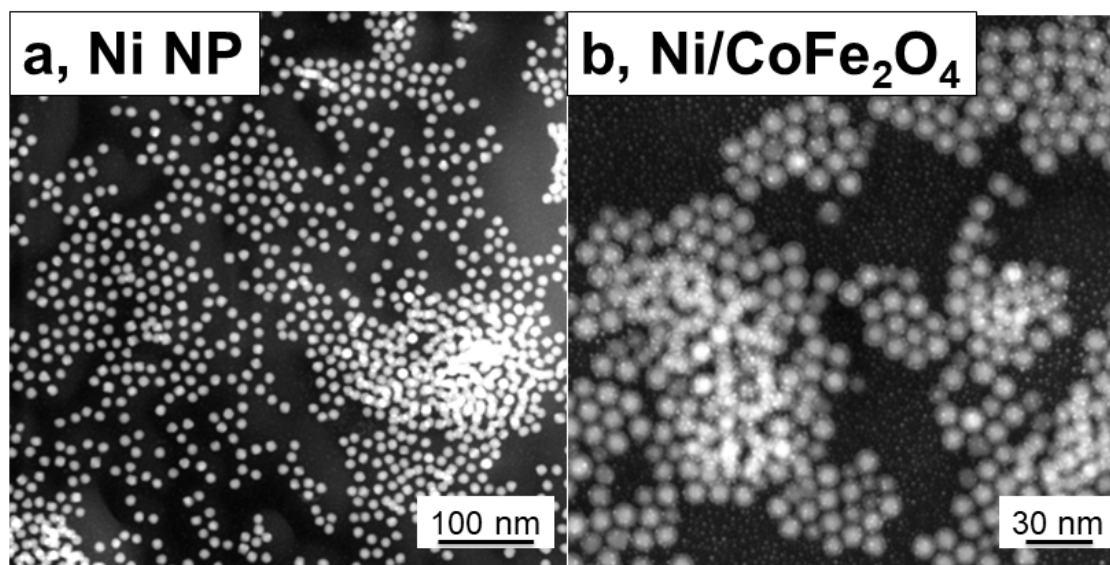


Figure S2. Representative HAADF image nanoparticles of (a) bare Ni and (b) Ni@CoFe₂O₄.

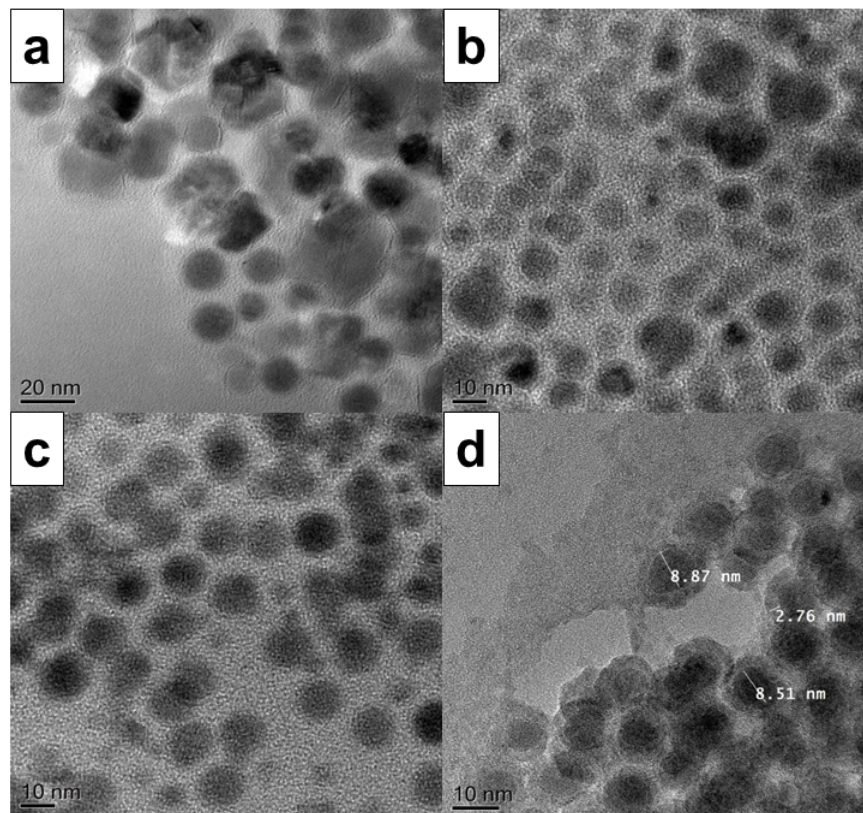


Figure S3. Representative TEM images of different synthetic conditions. (a) 12 mg Ni core with the addition of 0.11 mmol of $\text{Co}(\text{acac})_2$ and 0.22 mmol of $\text{Fe}(\text{acac})_3$ at 220 C reaction. (b) 20 mg Ni core with the addition of 0.11 mmol of $\text{Co}(\text{acac})_2$ and 0.22 mmol of $\text{Fe}(\text{acac})_3$ at 220 C reaction. (c) 50 mg Ni with 0.22 mmol of $\text{Co}(\text{acac})_2$ and 0.44 mmol of $\text{Fe}(\text{acac})_3$ at 220 C reaction. (d) Same conditions in the manuscript except the reaction temperature of 250 C.

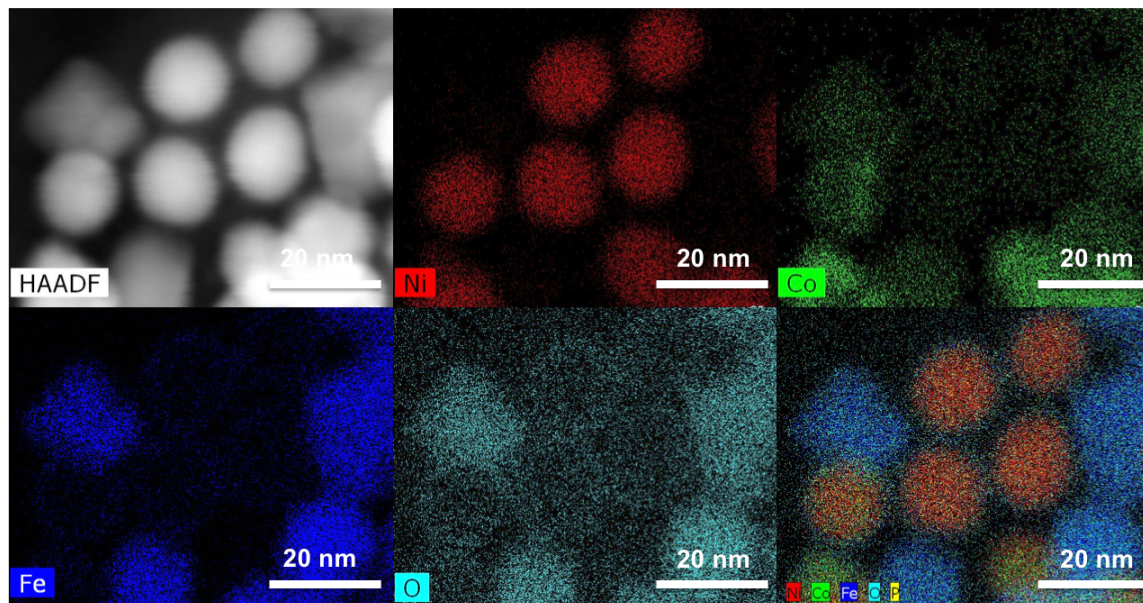


Figure S4. Representative images EDS mapping of Ni@CoFe₂O₄ nanoparticles, which is prepared by similar synthetic approaches attempted at temperatures without precursor decomposition; the synthetic conditions are following. 50 mg Ni core with the addition of 0.11 mmol of Co(acac)₂ and 0.22 mmol of Fe(acac)₃ at 250 C reaction.

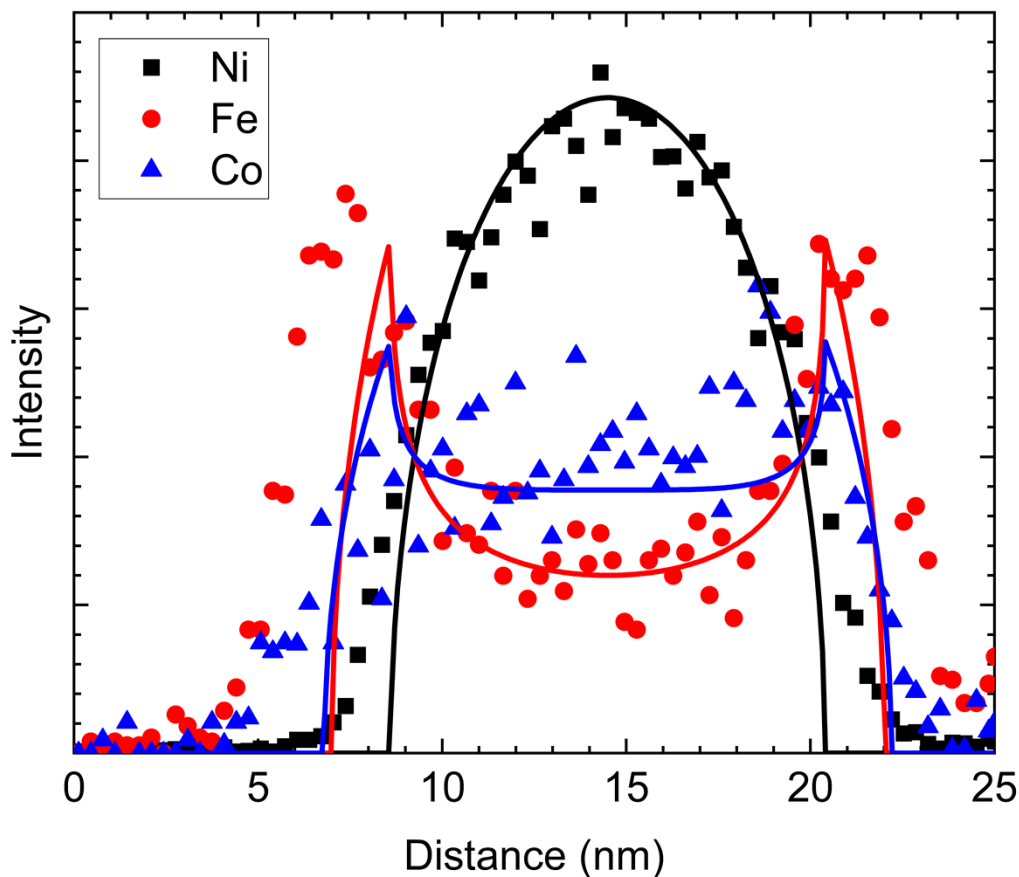


Figure S5. Modeling and analysis of linescans across the particles based on the result in Figure 1D. Points are data from the EDS linescan (for clarity only every 4th point is shown), solid lines are fits using the model described in the text. This model uses stoichiometric CoFe_2O_4 , and a 23% content of Co in the Ni core to reproduce the observed linescans. Here we have assumed equal yields from each element and an infinite penetration/escape depth, which is not strictly valid but simplifies analysis.

To estimate the composition of a core/shell nanoparticle line scan in Fig S5, the following functional forms were used where x in the third equation is the fraction of Co diffused into the Ni core:

$$Ni(r) = \begin{cases} 2r_1 \text{Sin}(\text{Arccos}(r/r_1)) & \text{if } |r| \leq r_1 \\ 0 & \text{if } |r| > r_1 \end{cases}$$

$$Fe(r) = \begin{cases} 2 \left[r_2 \text{Sin} \left(\text{Arccos} \left(\frac{r}{r_2} \right) \right) - r_1 \text{Sin} \left(\text{Arccos} \left(\frac{r}{r_1} \right) \right) \right] & \text{if } |r| \leq r_1 \\ 2r_2 \text{Sin} \left(\text{Arccos} \left(\frac{r}{r_2} \right) \right) & \text{if } r_1 \leq |r| \leq r_2 \\ 0 & \text{if } |r| > r_2 \end{cases}$$

$$Co(r) = \begin{cases} 2 \left[r_2 \text{Sin} \left(\text{Arccos} \left(\frac{r}{r_2} \right) \right) - (1-x)r_1 \text{Sin} \left(\text{Arccos} \left(\frac{r}{r_1} \right) \right) \right] & \text{if } |r| \leq r_1 \\ 2r_2 \text{Sin} \left(\text{Arccos} \left(\frac{r}{r_2} \right) \right) & \text{if } r_1 \leq |r| \leq r_2 \\ 0 & \text{if } |r| > r_2 \end{cases}$$

Here r_1 is the radius of the core of the particle, while r_2 is the total radius of the particle (core plus shell). A value of $x=0.23$ produced a functional form for the Ni, Fe, and Co line scans consistent with the experimental data shown in Figure 1.

This analysis follows that employed by Lavorato et al, [3] and is based on a functional form for the volume of the sphere under the electron beam. Note the implicit assumption that the interaction volume of the electrons covers the whole depth of the particle, and that the interfaces between the core and shell are perfectly sharp, with Co uniformly distributed in the core.

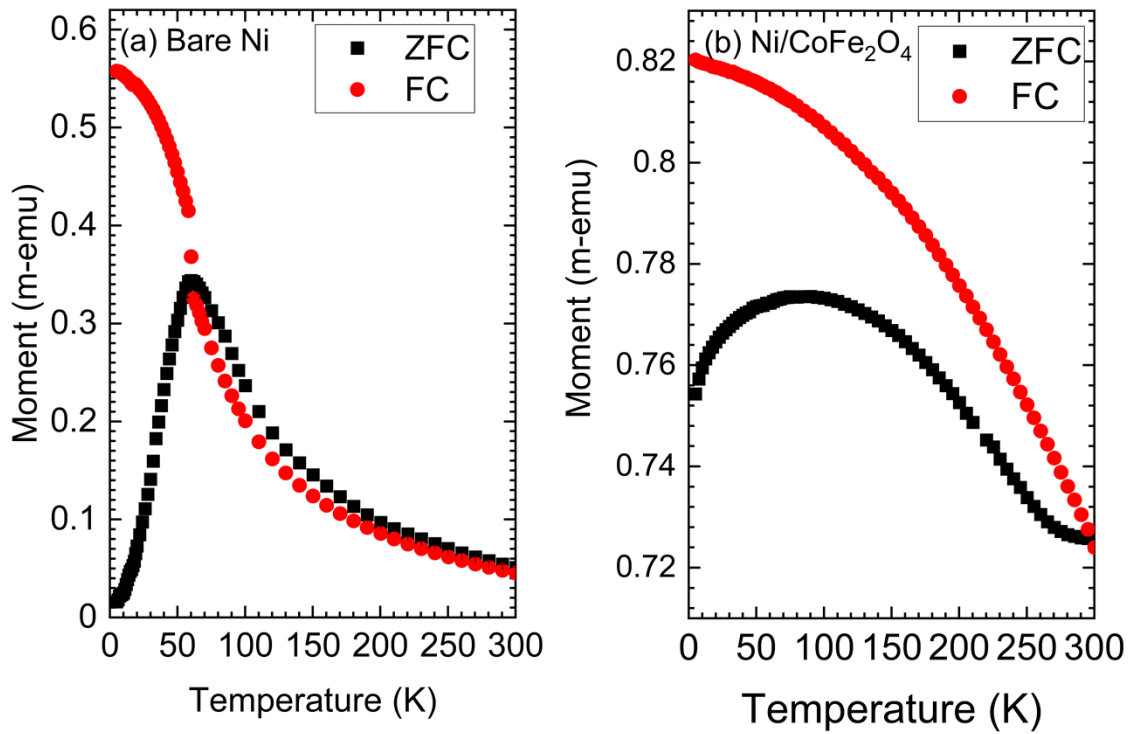


Figure S6: $M(T)$ data for bare Ni nanoparticles (left) and Ni/CoFe₂O₄ core-shell particles (right) measured in 50 Oe fields. A blocking temperature of ~ 60 K is visible in the Ni data, indicating superparamagnetic behavior, while the core-shell particles are ferromagnetic.

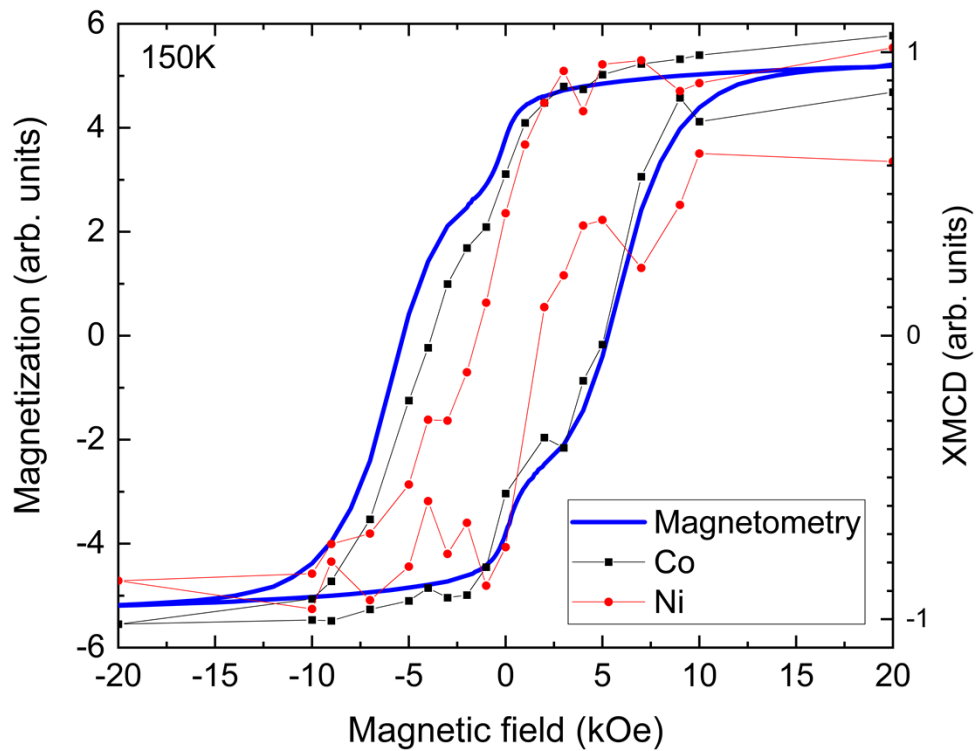


Figure S7: Bulk $M(H)$ data (solid blue line) and fluorescence-yield XMCD at the Co, Ni L_3 edges (connected points). The Ni shows a coercivity of approximately 1 kOe, and indications of two-stage switching, akin to the 80 K TEY data presented in Fig. 3. Note that the magnetometry data cannot be reproduced simply as a sum of Co and Ni plots, as data must be scaled for i) relative XMCD intensity and ii) presence of Fe, which was not measured here due to limited time.

Reference.

1. K. V. Chandekar, K. Mohan Kant, "Synthesis and characterization of low temperature superparamagnetic cobalt ferrite nanoparticles", *Adv. Mater. Lett.* 2017, 8, 435-443.
2. B. Liu, L. R. Liu, X. J. Liu, M. J. Liu and Y. S. Xiao, "Variation of crystal structure in nickel nanoparticles filled in carbon nanotubes", *Mater. Sci. Technol.* 2012, 28, 1345-1348.
3. G. C. Lavorato, A. A. Rubert, Y. Xing, R. Das, J. Robles, J. Litterst, E. Baggio-Saitovitch, M.H Phan, H. Srikanth, C. Vericat and M. H. Fonticelli, "Shell-mediated control of surface chemistry of highly stoichiometric magnetite nanoparticles" *Nanoscale.* 2020, 12, 12326-13636.